Colloid & Polymer Science Colloid Polym Sci 272:1536–1546 (1994)

Linear viscoelastic behaviour of complex polymeric materials: a fractional mode representation

Chr. Friedrich and H. Braun[1])

Institute of Macromolecular Chemistry and Freiburg Materials Research Center Albert-Ludwigs-University Freiburg i. Br. Freiburg i. Br., FRG
[1])Gebrüder HAAKE GmbH, Karlsruhe, FRG

Abstract: A rheological constitutive equation for complex polymeric materials is derived starting from a special formulation of the relaxation function. This relaxation function contains six parameters and is divided into three regions: the plateau region, an intermediate power-law region and the terminal region of rapid stress decay. Material functions like the complex modulus G^* and the logarithmic density function of the relaxation time spectrum H and of the retardation time spectrum L respectively are derived. Material parameters like the zero shear viscosity η_0 and the equilibrium shear compliance J_e are also calculated. The comparison of the measured dynamic moduli of H-shaped polystyrenes, associating terminally functionalized polyisoprenes and randomly associating polybutadienes with the theoretical predictions of the proposed phenomenological model shows an excellent agreement.

Key words: Rheological constitutive equation – fractional derivatives – material functions – relaxation time spectra – retardation time spectra

I. Introduction

There is a large variety of polymeric materials showing relaxational behavior in the plateau and flow regions that is quite different from linear, monodisperse polymers. Polybutadienes modified by urazole groups and interacting via H-bridges [1–5] belong to this group as well as H-shaped polystyrenes [6, 7] and endfunctionalized polyisoprenes [8]. The well known relaxational behavior of linear monodisperse polymers, expressed by the frequency dependency of the storage modulus G' and loss modulus G'', is characterized by a very fast transition from the plateau region ($G' \propto G_0\omega^0$, G_0 is the plateau modulus) into the flow region ($G' \propto \omega^2$, $G'' \propto \omega$). In contrast to this, the measured G' and G'' curves for the materials under consideration here, show *three* relaxation zones: the plateau region for $\omega > t_0^{-1}$, a power-law region for $t_m^{-1} < \omega < t_0^{-1}$ and the flow region for frequencies smaller than t_m^{-1}. The two time parameters t_0 and t_m characterize the width of the power law zone. In this zone, the material functions G' and G'' depend on frequency in the following way: $G' \propto \omega^\alpha$ and $G'' \propto \omega^\beta$, where α and β assume values between 0 and 1. The quantitative description of such a behavior should be based on a relaxation function, $G(t)$, which is composed of three parts:

$$G(t) = \begin{Bmatrix} G_0 f_1(t) & t < t_0 \\ G_0 f_2(t) & t_0 < t < t_m \\ G_0 f_3(t) & t > t_m \end{Bmatrix} \tag{1}$$

G_0 is the plateau modulus. The function f_1 is equal to one or a slightly decreasing function describing the plateau. The function f_2 is of power law type with a power α between zero and one. $f_3 \propto \exp(-t/t_m)$ describes the cut-off of the relaxation processes.

Recently [9, 10], a six parametric phenomenological relaxation function was formulated which reflects this observed behavior:

$$g(t) = \frac{G(t) - G_\mathrm{e}}{G_0 - G_\mathrm{e}} = x_0^{q-1} E_{a,q}(-x_0^a)\exp(-x_\mathrm{m}) \,, \tag{2}$$

where $q = a - r$, $r = b - 1$, $x_0 = t/t_0$, $x_\mathrm{m} = t/t_\mathrm{m}$ and G_e is the equilibrium modulus. In this equation, $E_{a,q}$ is the generalized Mittag–Leffler function. Its behavior is described by Bateman [11] in more detail. The first two terms on the right-hand side of this function are the relaxation function of the Fractional Standard Solid Model [12–14] (FSSM). In analogy to Maxwell modes, we will call them fractional modes. The most important feature of this mode consists in its double power-law behavior. From the asymptotic expansion of this part of the relaxation function follows that g_FSSM is proportional to $x_0^{\mathrm{a}-\mathrm{b}}$ for $t < t_0$ (intermediate region) and $g_\mathrm{FSSM} \propto x_0^{-\mathrm{b}}$ for $t > t_0$ and $b < 1$ (plateau region). Thermodynamic admissibility requires the relationship $0 < a \leq \mathrm{b} \leq 1$ for the power-law parameters [12, 13]. The introduced cut-off function, $\exp(-x_\mathrm{m})$, guarantees the fast release of stresses within the material. This phenomenological procedure introduces "fluid behavior" into the model.

In a previous paper [10] the components of the complex modulus were derived from Eq. (2). These material functions are given once more here for reasons of completeness in the material functions paragraph. So far, the usefulness of the ansatz (2) was demonstrated only by one example (modified polybutadiene (PB265)). However, power laws are widely used in material sciences to describe self-similar structures which are independent of the physical details composing this structure [16]. So, it should be possible to also describe other materials (chemically and physically crosslinked polymers) using this formula.

It is the aim of this paper to derive the complete rheological model. That means that we will give further material functions (the logarithmic density function of the relaxation time spectrum and the density function of the retardation time spectrum) and material parameters (equilibrium compliance, Newtonian viscosity). Later, we want to show by the example of a distinct number of materials that this model is able to well describe quantitatively the material functions for different polymers with different molecular structure. The rheological constitutive equation is also derived to give a first physical interpretation of this phenomenological model.

II. Material functions

A. Complex modulus

In the following, the components of the complex modulus are given as derived in [10]. These equations yield the components of the complex moduli, G' and G'', in their dimensionless forms, g_1 and g_2, respectively.

$$g_1 = \frac{G' - G_\mathrm{e}}{G_0 - G_\mathrm{e}} = \omega t_0 \frac{(\omega^2 t_0^2 + w^2)^{(r+a)/2} \sin(q\,\varphi) - (\omega^2 t_0^2 + w^2)\sin(r\,\varphi)}{1 + 2(\omega^2 t_0^2 + w^2)^{a/2}\cos(a\,\varphi) + (\omega^2 t_0^2 + w^2)^a} \tag{3a}$$

$$g_2 = \frac{G''}{G_0 - G_\mathrm{e}} = \omega t_0 \frac{(\omega^2 t_0^2 + w^2)^{(r+a)/2} \cos(q\,\varphi) + (\omega^2 t_0^2 + w^2)\cos(r\,\varphi)}{1 + 2(\omega^2 t_0^2 + w^2)^{a/2}\cos(a\,\varphi) + (\omega^2 t_0^2 + w^2)^a} \tag{3b}$$

Here, the following notation is used: $\varphi = \arctan(\omega t_\mathrm{m})$ and $w = t_0/t_\mathrm{m}$. It can be proven that for $t_\mathrm{m} \to \infty$ and $a = b = 1$ Eqs. (3a) and (3b) yield the well known results of the Maxwell model. The principal behavior of g_1, Eq. (3a), is shown in Fig. 1 for different a, b and w-values. The three regions and the corresponding characteristic times are separated very well.

The components of the complex compliance $J^* = J' + iJ''$ can be determined from the complex modulus by the well known inversion formula: $J^* = G^{*-1}$. This formula leads to the following relationships between the components: $J' = G'/(G'^2 + G''^2)$ and $J'' = G''/(G'^2 + G''^2)$. So, it seems to be not necessary to give the individual formulas of each component.

B. Relaxation time spectrum

It is also of interest to calculate the density function of the relaxation time spectrum in order to show how the relaxation times are distributed. In this way, one gets an idea about the interpretation of the model and material parameters.

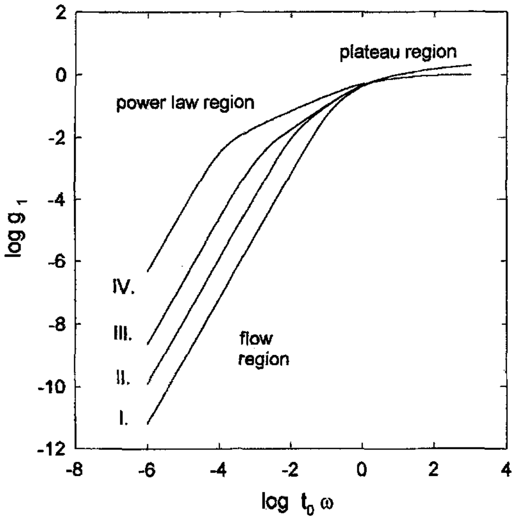

Fig. 1. Model predictions for the dimensionless storage modulus g_1 dependent on the dimensionless frequency ωt_0. The curves I to IV correspond to the following parameter sets: I.: $a = 0.6$, $b = 0.7$, $w = 0.1$; II.: $a = 0.6$, $b = 0.7$, $w = 0.01$; III.: $a = 0.6$, $b = 0.7$, $w = 0.001$; IV.: $a = b = 0.5$, $w = 0.0001$

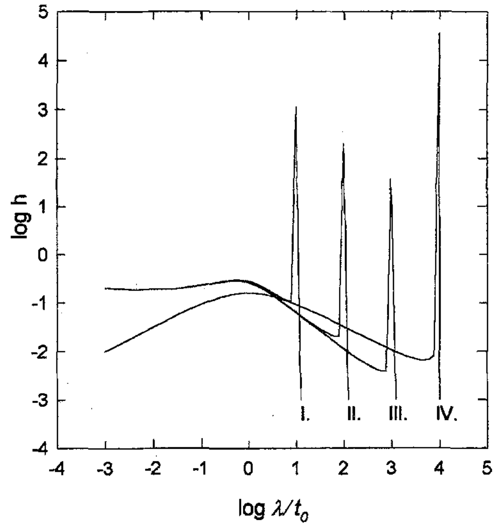

Fig. 2. Model predictions for the dimensionless density function of the relaxation time spectrum h depending on the dimensionless relaxation time λ/t_0. The curves I. to IV. correspond to parameter sets given in Fig. 1

In principle, the relaxation function and the density function are related by a Laplace transform. However, often it is very complicated to calculate the inverse transform of the relaxation function. For that reason, another method – the inverse Stieltjes transformation (for details see Tschoegl's textbook [17]) – is used. In this way, one obtains the following equation relating the density function with the relaxance:

$$H(\lambda) = \pm\frac{1}{\pi}\lim_{\varepsilon\to 0}\operatorname{Im}\{Q(s)_{s=-1/\lambda\pm i\varepsilon}\}\,. \tag{4}$$

According to Tschoegl, the relaxance is the quotient of the Laplace transform of the stress $L[\tau] = \bar{\tau}$ and the Laplace transform of the deformation $L[\gamma] = \bar{\gamma}$, $Q(s) = \bar{\tau}/\bar{\gamma}$. For $a \le b < 1$, Eq. (4) together with Eq. (3) yields the expression for the dimensionless density function $h(u)$:

$$h(u) = \frac{H(\lambda)}{G_0 - G_e} = \begin{Bmatrix} h_0(u), & u < w^{-1} \\ 0, & u \ge w^{-1} \end{Bmatrix}, \tag{5a}$$

with

$$h_0(u) = \frac{1}{\pi}\,\frac{(1-wu)^r u^{a-b}[u^a\sin(b\pi) + (1-wu)^a\sin((b-a)\pi)]}{u^{2a} + 2\cos(a\pi)u^a(1-wu)^a + (1-wu)^{2a}} \tag{5b}$$

and $u = \lambda/t_0$.

A plot of the density function for different a and b is given in Fig. 2. From that example it is evident that the time parameter t_m is the longest relaxation time inherent in this model. If $t_m \to \infty$, the presented relaxation time spectrum yields the spectrum for the generalized Cole–Cole behavior [14].

C. Retardation time spectrum

The logarithmic density function of the retardation time spectrum $L(\lambda)$ is defined in analogy to Eq. (4) in the following way:

$$L(\lambda) = \mp\frac{1}{\pi}\lim_{\varepsilon\to 0}\operatorname{Im}\{U(s)_{s=-1/\lambda\pm i\varepsilon}\}\,, \tag{6}$$

Where U is the so-called retardance and given as Q^{-1}. Using the same procedure as described for the derivation for the relaxation time spectrum, we end up with the dimensionless density function

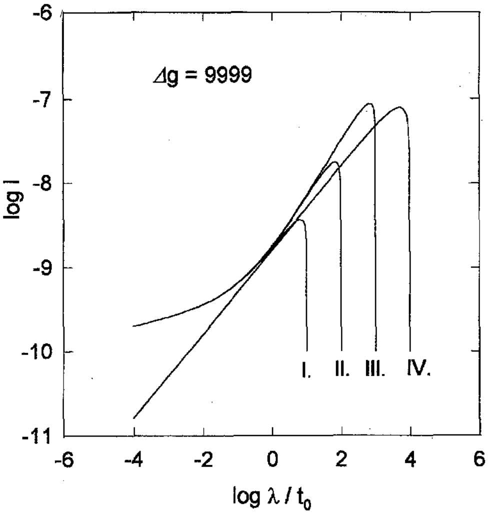

Fig. 3. Model predictions for the dimensionless density function of the retardation time spectrum 1 depending on the dimensionless retardation time λ/t_0. The curves I to IV correspond to parameter sets given in Fig. 1. $\Delta g = (G_0 - G_e)/G_e$

of the retardation time spectrum $l(u)$:

$$l(u) = \frac{L(\lambda)G_e^2}{(G_0 - G_e)} = \begin{Bmatrix} l_0(u), & u < w^{-1} \\ 0, & u \geq w^{-1} \end{Bmatrix}, \tag{7a}$$

with

$$l_0(u) = \frac{1}{\pi} \frac{u^{a-b} z^r [u^a \sin(b\pi) + z^a \sin((b-a)\pi)]}{u^{2a} + 2\cos(a\pi) u^a z^a + z^{2a} + \Delta g u^{a-b} z^r \{2u^a \cos(b\pi) + 2z^a \cos((b-a)\pi) + \Delta g u^{a-b} z^r\}}; \tag{7b}$$

$z = 1 - wu$ and $\Delta g = (G_0 - G_e)/G_e$. A plot of the retardation time spectrum for different a, b and w-values is given in Fig. 3. In this case, the same parameter combinations are used as for the calculation of the relaxation time spectrum given in Figs. 1 and 2.

III. Material parameters

Important material parameters like the zero shear rate viscosity η_0 and the equilibrium shear compliance J_e are calculated in this section. Compared to the plateau modulus G_0, these parameters are not included in the model directly. On the one side, the knowledge of these parameters is important to use this model. On the other side, it is also important to derive the interrelation between material parameters which act as consistency relations. It is known for star-shaped polymers [18], for example, that the product of equilibrium compliance and Newtonian viscosity is half the longest relaxation time.

While the Newtonian viscosity is the zeroth momentum of the relaxation function, the equilibrium compliance is the ratio of the first momentum and the square of the zeroth. The calculation of both momentum yields the desired material parameters in dimensionless form:

$$\frac{\eta_0}{G_0 t_m} = \frac{w^b}{1 + w^a}, \tag{8}$$

and

$$J_e G_0 = q w^{a-b} - r w^{-b}. \tag{9}$$

Equation (8) is the dimensionless viscosity scaled by the product of the longer of both times and the plateau modulus. A second dimensionless viscosity which is scaled by the shorter of both times can also be given using the relation $w = t_0/t_m$. The dimensionless viscosity (8) depends on the ratio of the characteristic times and the exponent a and b. However, it depends only on w and b in the relevant range $w \ll 1$.

A similar behavior is observed for the dimensionless equilibrium shear compliance, Eq. (9), scaled with the plateau modulus. A second equation is here also of interest. In this case the equilibrium compliance is scaled with the term η_0/t_m. This expression yields a constant value, $1 - b$, in the interesting range of w-values $w \ll 1$.

IV. Rheological constitutive equation

Now, the corresponding rheological equation will be derived. This equation is important for the physical interpretation of the proposed relaxation function. Similar to the Maxwell model, where the quantities can be interpreted at least in terms of a mechanical analogue, we derive the constitutive equation in the hope of finding a similar interpretation. The starting point for the derivation is the relaxance. The rheological constitutive equation can be found by inverting this relation, i.e., by calculating the inverse Laplace transform. This was done by Friedrich [10], who arrived at:

$$\tilde{\tau} + t_0^a \mathrm{e}^{-t/t_\mathrm{m}} D^a[\tilde{\tau}\mathrm{e}^{t/t_\mathrm{m}}] = (G_0 - G_\mathrm{e}) \times t_0 t_0^{b-1} \mathrm{e}^{-t/t_\mathrm{m}} D^{b-1}[\dot{\gamma}\mathrm{e}^{t/t_\mathrm{m}}] \,, \tag{10}$$

where D^a is the fractional derivative of order a and $\tilde{\tau}$ is a reduced stress tensor: $\tilde{\tau} = \tau - G_\mathrm{e}\gamma$. This equation, which contains an apparent ~~uncertain~~ty, was the final result in Friedrich's derivation. There is an explicit time dependence which should not exist for a chemically equilibrated material. So, Eq. (10) cannot be the final version of a rheological constitutive equation corresponding to the relaxation equation (2). We will remove this explicit time dependence using the product rule for fractional differential operators [19] which is a generalization of the integer order rule and given by Eq. (11).

$$D^c[rs] = \sum_{j=0}^{\infty} \binom{c}{j} D^j[r] D^{c-j}[s] \tag{11}$$

In this way, the rheological constitutive equation (10) can be transformed into the following expression:

$$\tilde{\tau} + w^a \sum_{j=0}^{\infty} t_{\mathrm{m}aj}^{a_j} D^{a_j}[\tilde{\tau}] = (G_0 - G_\mathrm{e}) t_0 w^r \times \sum_{j=0}^{\infty} t_{\mathrm{m}bj}^{b_j} D^{b_j}[\dot{\gamma}] \,, \tag{12}$$

with

$$t_{\mathrm{m}bj} = \binom{b-1}{j}^{1/b_j} t_\mathrm{m}, \quad b_j = b - 1 - j$$

$$t_{\mathrm{m}aj} = \binom{a}{j}^{1/a_j} t_\mathrm{m}, \quad a_j = a - j$$

Due to the fact that a_j and b_j become negative for $j > 1$, this constitutive equation contains fractional derivatives as well as fractional integrals. From the mathematical point of view, both equations (10) and (12) are equivalent. Nevertheless, Eq. (12) is more convenient because it is closer to the well known equations (like the Maxwell model) in mathematical structure. The latter can be obtained by setting $a = b = 1$ and $t_\mathrm{m} \to \infty$. In this case, only the first term of the sums remains and yields the well known Maxwell model.

The presented rheological constitutive equation transforms to the Fractional Maxwell Model (12a) for $t_\mathrm{m} \to \infty$ and arbitrary a and b fulfilling conditions $0 < a \leq b \leq 1$.

$$\tilde{\tau} + t_0^a D^a[\tilde{\tau}] = (G_0 - G_\mathrm{e}) t_0^b D^b[\gamma] \tag{12a}$$

This type of constitutive equation was investigated in more detail in [12, 13, 15]. Very recently, Glöckle and Nonnenmacher [25] showed the close interrelation between a special case of this equation ($a = b$) and some specific statistics used for the description of relaxation processes in polymeric materials. We will stress this problem in more detail in section VI.

The other limiting case, $t_0 \to 0$ leads together with Eq. (8) for fluid behavior to Eq. (12b).

$$\tilde{\tau} = \eta_0 \sum_{j=0}^{\infty} t_{\mathrm{m}bj}^{b_j} D^{b_j}[\dot{\gamma}] \,. \tag{12b}$$

This type of equation with $j = 0, 1$ was used to describe the rheology of a crosslinking PDMS [21]. The relationship of this model to the Rouse behavior was discussed in [24].

Our constitutive equation belongs to the class of linear viscoelastic models. The Fractional Maxwell (or Standard Solid) Model was the starting point and no geometric nonlinearity was introduced. Nonlinear responses can be described when, for example, the material functions are made deformation dependent in some specific manner. But this is not the task of the present paper. It should also be mentioned that this generalized Fractional Maxwell Model is, as well as the Maxwell Model itself, not objective with respect to the invariance against coordinate transformations. But there is no loss of generality because the use of the model is restricted, as mentioned, to deformation histories with small deformation amplitudes.

V. Comparison: theory experiment

In the following, the usefulness of the presented model is tested by the example of the usefulness of its material functions. For that purpose, the material behavior corresponding to Eq. (3) is compared with experimental results obtained from different polymeric systems: A) H-shaped polystyrenes, B) associating polybutadiens, and C) a zwitterionic polyisoprene. The measured G' and G'' of all these materials are given in Figs. 4 to 8 by open symbols.

Table 1. Material parameters according to Eq. (3) for different H-shaped polystyrenes

Material	$\log t_m$, s	$\log t_0$, s	$\log G_0$, Pa	a	b	a_{gl}	$\log G_{gl}$, Pa
H2A1	0.42	− 1.05	6.26	0.593	0.652	0.634	4.19
H1A1	2.45	− 0.24	6.25	0.554	0.554	0.548	4.53
H5A1	3.94	0.71	6.33	0.397	0.397	0.589	4.35

Table 2. Material parameters according to Eq. (3) for different polybutadienes and a zwitterionic polyisoprene

Material PB	$\log t_m$, s	$\log t_0$, s	$\log G_0$, Pa	a	b
260	− 1.56	− 2.51	5.58	0.864	0.997
2605	− 0.72	− 2.21	5.43	0.786	0.932
262	0.78	− 1.17	5.43	0.758	0.894
265	2.71	0.19	5.40	0.687	0.849
267	4.15	1.06	5.48	0.590	0.760
200	0.69	− 0.76	4.91	0.886	0.993
202	3.40	− 0.91	5.00	0.501	0.604
204	4.47	0.92	4.91	0.517	0.614
Zwi-IP	1.74	− 0.64	5.34	0.475	0.607

In order to determine the model parameters, fits for G' and G'' are performed using Eqs. (3a) and (3b). The parameters for the H-shaped polystyrenes are given in the Table 1 and for the polybutadiens and the polyisoprene in Table 2. A second term, $G_{gl}(i\omega)a_{gl}$, was added to Eqs. (3) and included in the procedure for the H-polymers. This is necessary to model the transition from the plateau modulus towards the glass region.

In order to describe the discussed behavior of associating and H-shaped polymers qualitatively and quantitatively, five parameters are necessary. The number of parameters corresponds to the number of characteristic mathematical features of a material function. The plateau modulus G_0 describes the "height" of the moduli functions, the two time parameters t_0 and t_m the position of the characteristic "kinks" on the time scale and the "width" of the intermediate power-law region. Two additional parameters, a and b, are necessary to model the slopes of the curves in the power-law region as well as in the plateau region. The latter region is indeed of power-law type and one needs a slope different from zero in order to get a good quantitative description of the plateau. This is an experimental observation for materials with low and intermediate molecular weights ($M > M_e$).

The model parameters can only be determined with a certain accuracy. This accuracy depends on the separation of the different regions and the location of it within the experimental window. The question of parameter uncertainty will be discussed by the example of H-shaped PS and Stadler's PB.

A. H-*shaped polystyrene*

The first system consists of three samples of H-shaped polystyrenes, H2A1, H1A1 and H5A1, with molecular weights M_n of 237, 483 and 1040 kg/mol, respectively. For a more detailed description of material behavior consult [6]. The comparison between the parameters determined by our fit and that given in [6] is presented in Table 3. The results are presented in Fig. 4. Roovers determined the zero shear rate viscosity as the limit of the ratio G'' to ω for vanishing frequencies. The equilibrium shear compliance is determined as the ratio ψ_{10}/η_0^2 where the initial coefficient of the first normal stress difference

Table 3. Comparison of material parameters determined by different methods

	$\eta_0 \cdot 10^{-5}$,	Pas	$G_0 \cdot 10^{-6}$	Pa	$J_e \cdot 10^6$	Pa^{-1}
Material	Roovers	Eq. (8)	Roovers	Directly from fit	Roovers	Eq. (9)
H2A1	5.1	5.26	2.1	1.82	2.3	2.37
H1A1	170	163	1.9	1.78	8.3	8.4
H5A1	≈ 6000	9713	1.9	2.14	–	9.41

ψ_{10} is calculated from the limit of the ratio G' to ω^2 for vanishing frequencies. The plateau modulus is the $2/\pi$ multiplied area under the curve G''/ω. Our procedure allows to easily find the desired material parameters by fitting the corresponding equations to the experimental data.

Figure 4c shows that the accuracy of this parameter determination may not be high. From Figs. 4a and b it is obvious that in the case of H5A1 the onset of the flow region is not well represented by the data. This leads to a relative large error in the determination for both time parameters. The error for the viscosity is even larger. Nevertheless, this procedure of parameter determination via the proposed model gives an estimate of the desired parameters with the corresponding error.

B. Associating polybutadienes

The second group of materials belongs to urazole modified polybutadienes. These data are obtained from the literature [1–4] and [5]. Here, the pure polybutadiene ($M_w = 26$ kg/mol for Stadler's data and 42 kg/mol for Odenwald's data) and modifications with 0, 0.5, 2, 5, 7 and 0, 2, 4 mol% resp. urazole are considered. The data of Odenwald are included because they demonstrate clearly that the addition of urazole modifies the long time behavior of these materials in a manner as proposed by this model. Both data sets on PB's are not directly comparable because of the different architecture of the monomer units in these materials.

The model calculations agree very well with the experimental data. These results are shown in Figs. 5 and 6. Stadler gives for his PBs a plateau modulus which increases in dependence on the degree of modification from 600 to 900 kPa. Our results support a modification independent plateau modulus with a value of about 300 kPa. The determination of the plateau modulus using the integration procedure of the η'-curve is connected

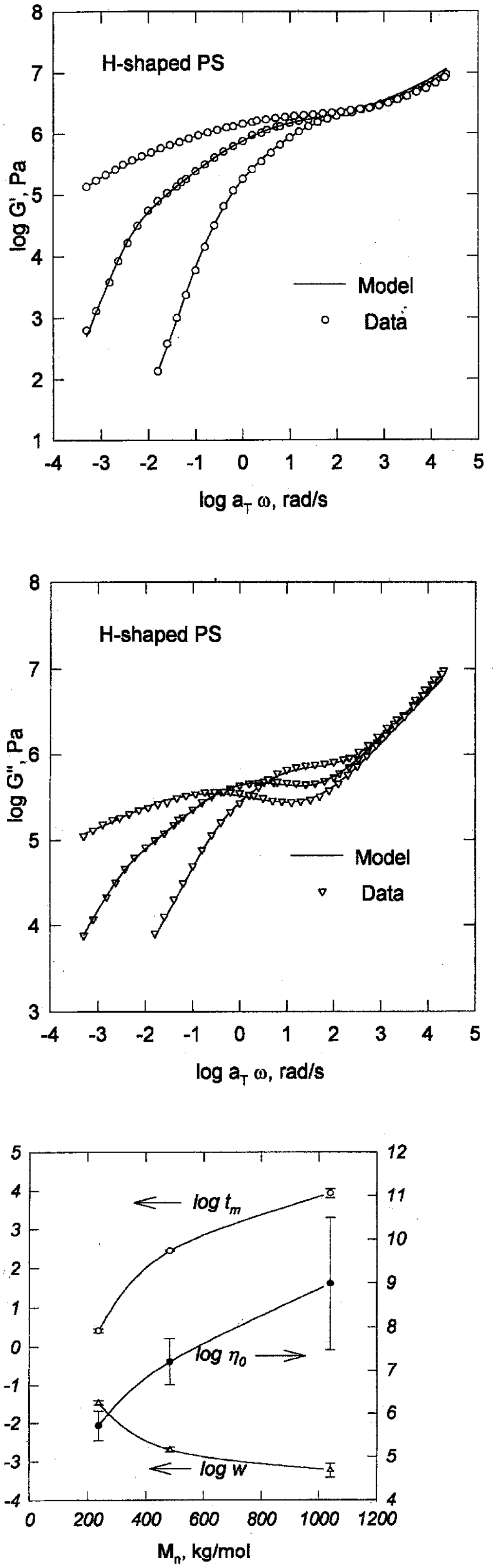

←

Fig. 4. Dependence of the storage modulus $G'(a)$ and the loss modulus $G''(b)$ from the reduced frequency for three different H-shaped polystyrenes with molecular weights M_n of 237 kg/mol (H2A1), 483 kg/mol (H2A1) and 1040 kg/mol (H5A1) respectively. The data are of J. Roovers. (c) shows the dependence of t_m, η_0, and w and the corresponding error bars on the molecular weight. The lines are drawn to guide the eyes

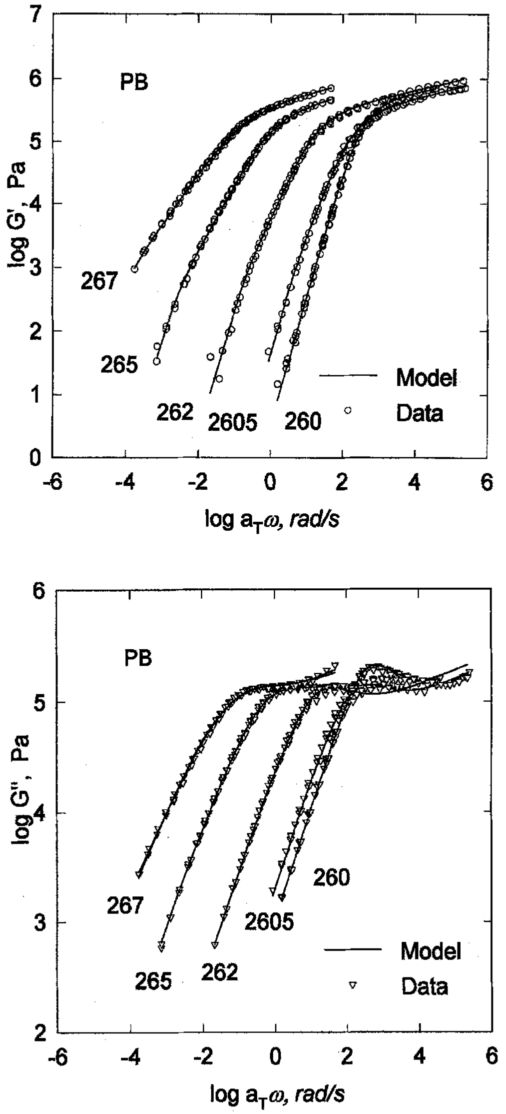

Fig. 5. Dependence of the storage modulus $G'(a)$ and the loss modulus $G''(b)$ from the reduced frequency for unmodified and urazole modified polybutadienes with a molecular weight M_w of 26 kg/mol. The lines correspond to the fits performed with Eq. (3). The data are of R. Stadler and L. de Lucca-Freitas

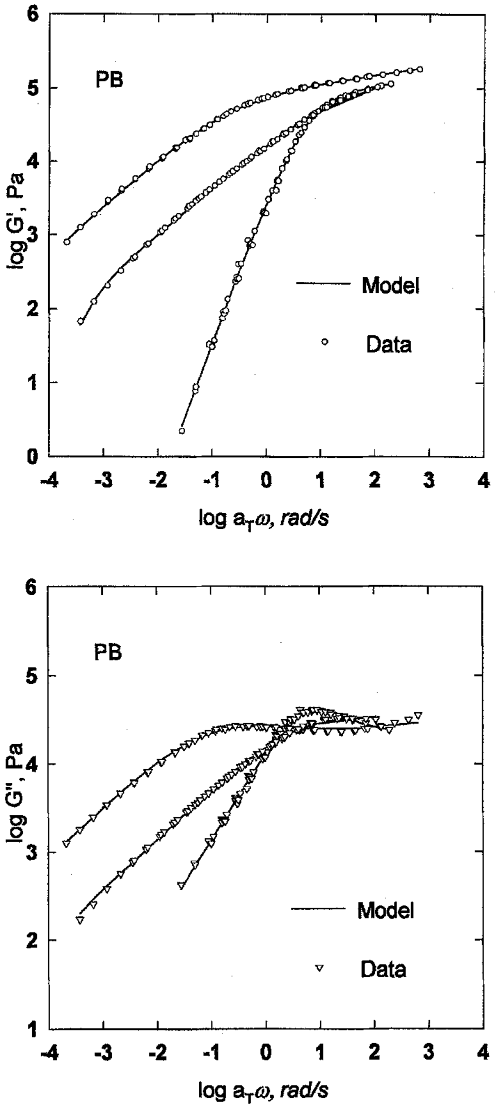

Fig. 6. Dependence of the storage modulus $G'(a)$ and the loss modulus $G''(b)$ from the reduced frequency for unmodified and urazole modified polybutadiene with a molecular weight M_w of 42 kg/mol. The data are of Odenwald

with a certain inaccuracy. So, the agreement between these results is sufficient. The invariance of the plateau modulus with increasing amounts of modifiers is also supported by the measurements of Odenwald. The difference between both time constants becomes very significant with increasing modification. The power law exponents tend to fall from values near to one (for monodisperse polymers) to values near a half. These tendencies seem to be an indicator for the increasing molecular polydispersity. This picture is consistent with that known from the sol-gel transition. At the gel point, t_m should be infinite, t_0 remains finite and the slope of the curve is in the range of 0.5 to 0.7 in dependence on the stoichiometry of the polymers [20, 21].

Figure 7 gives the dependency of some material parameters and dimensionless complexes on the

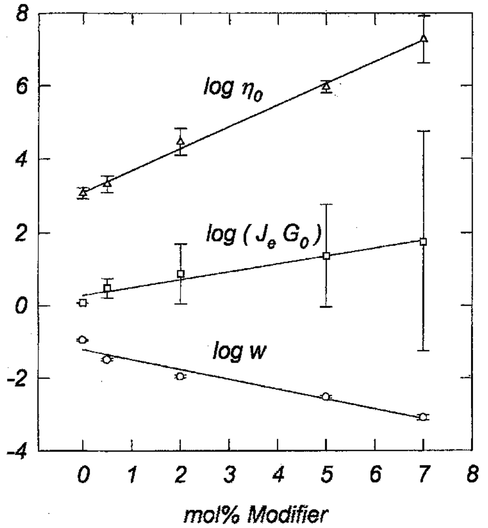

Fig. 7. Dependence of different material parameters on the degree of modification for the polybutadienes of R. Stadler and L. de Lucca-Freitas. The lines correspond to a regression of first order

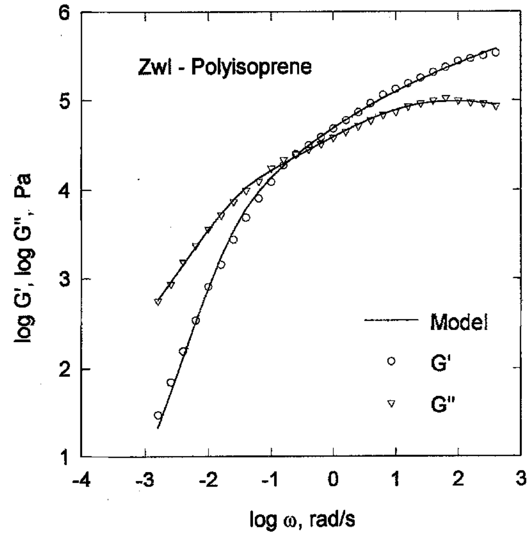

Fig. 8. Dependence of the storage modulus G'(o) and the loss modulus G'' from the frequency for a zwitterionic polyisoprene with a molecular weight M_w of 237 kg/mol. The data are of Fetters et al

degree of modification of Stadler's PB. Once more, this figure shows also the errors of the primary data (here t_m) and the errors of the derived material parameters. Again, the errors are large if the regions which determine the corresponding parameters are not fully within the experimental attainable window. For the highest degree of modification it is difficult to determine t_m and to derive η_0.

C. Zwitterionic polyisoprene

The last example is from Fetters and coworkers [8] and represents a monofunctional zwitterionic polyisoprene with a molecular weight of 107 kg/mol. This material is also described very well by our equations, as can be seen from Fig. 8. In general, the material parameters are closer to that of H-shaped PS than to the PBs. Perhaps, this is an indication for a molecular structure similar to that of the Hs.

VI. Discussion and Conclusions

We presented material functions and material parameters belonging to a relaxation function composed of three parts: a plateau region, a flow region, and an intermediate power law region. This last region represents the peculiarity occurring in the rheological response of distinct polymers. Our model includes the necessary number of parameters and describes this intermediate power law region. The comparison of experimental data with the calculated curves shows that the agreement between theory and experiment is excellent for all materials considered here. In general, it seems that Eq. (3) qualitatively and quantitatively correctly describes the rheological behavior of the materials under consideration.

A closer look at the material parameters and the analysis in dependence of the w-value seems to be helpful to interpret the meaning of the time parameters. A combination of Eqs. (8) and (9) yields:

$$\frac{\eta_0 J_e}{t_m} = \frac{q w^a - r}{1 + w^a}, \tag{9a}$$

It is well known that the product of the equilibrium compliance and the Newtonian viscosity represents the weight-average relaxation time [23]. The analysis of Eq. (9a) shows that the right-hand side of this equation is nearly independent of w. That means that t_m is related to λ_w in the following manner: $t_m = \text{const}\, \lambda_w$.

A similar relation cannot be found for t_0 and λ_n. Nevertheless, the analysis of Eq. (9) helps us to establish a relationship between the ratio of both model time parameters, w, and the ratio λ_w/λ_n, where λ_w is the weight-average relaxation time according to Ferry:

$$\frac{\lambda_w}{\lambda_n} = \text{const}\left(\frac{t_m}{t_0}\right)^b , \tag{9b}$$

where const is of order $1 - b$ for w-values less than 0.01. This analysis explains that the complex w^{-b} can be treated as the ratio of the weight to the number average relaxation times.

It would also be of interest to compare different material functions for one material. Due to the lack of appropriate experimental data, a comparison must be performed in the future.

Finally, we have to discuss the physical interpretation of the obtained rheological constitutive equation. The most significant disadvantage of our model is its phenomenological character. However, this inconvenience is common to all rheological constitutive equations with fractional derivatives or integrals. Recently, Schiessel and Blumen [22] used so-called ladder models (i.e., special arrangements of springs and dashpots) for an explanation of the simple Fractional Maxwell (or Fractional Standard Solid) Model. They found that each fractional derivative leads to a ladder-like structure with an infinite number of springs and dashpots. So, a mechanical analogue was found, which is a first step towards its physical interpretation. The Fractional Maxwell Model corresponds to our model in the plateau and power law regions. On the other hand, the model (12) behaves like model (12b) for times $t \approx t_m$ and longer. The summation over fractional derivatives of the strain or strain rate corresponds to a parallel arrangement of ladders due to the fact that relaxances add in parallel [17]. So, the model structure changes from a series representation of only two ladders (fractional modes) to a parallel presentation of an infinite number of ladders.

However, the mechanical model representation gives only a limited insight into the physics behind the fractional modes. From that point of view, the considerations of Bagley and Torvik [24] and Glöckle and Nonnenmacher [25] are more helpful. In [24] it was pointed out that a model based on Eq. (12b) with $j = 0$ and $b = 1/2$ is equivalent to the Rouse behavior. These authors could show that this type of model is consistent with the predictions of molecular theories. On the other hand, this approach gives no hints about the "molecular origins" of fractional derivatives.

In contrast, Glöckle and Nonnenmacher showed that a specific case ($a = b$) of Fractional Maxwell model is a natural consequence of molecular processes with a certain statistics. They could show that Continuous Time Random Walks with Levy-type waiting time distributions lead to constitutive equations with fractional derivatives. This seems to be the most promising concept for an improved understanding of such constitutive equations.

References

1. Stadler R, deLucca-Freitas LL (1986) Progr Colloid Polym Sci 64:773–778
2. Stadler R (1987) Progr Colloid Polym Sci 75:140–145
3. Stadler R, deLucca-Freitas LL (1989) Macromolecules 22:714–719
4. deLucca-Freitas LL, Stadler R (1987) Macromolecules 20:2478–2485
5. Odenwald M (1992) Diploma Thesis, Freiburg i.Br
6. Roovers J (1984) Macromolecules 17:1196–1200
7. Roovers J (1985) Polymer 26:1091–1095
8. Fetters LJ, Graessley WW, Hadjichristidis N, Kiss AD, Pearson DS, Younghouse LB (1988) Macromolecules 21:1644–1653
9. Friedrich Chr (1992) In: Moldenaers P, Keunings R (eds) Theoretical and Applied Rheology. Elsevier, Amsterdam, 91–93
10. Friedrich Chr (1992) Phil Mag Letters 66:287–292
11. Bateman H (1955) Higher Transcendental Functions vol 3. McGraw Hill, New York
12. Friedrich Chr (1991) Rheol Acta 30:151–158
13. Friedrich Chr (1991) Lecture Notes in Physics No. 38. Springer, Berlin, Heidelberg, New York, pp 321–330
14. Friedrich Chr, Braun H (1992) Rhoel Acta 31:309–322
15. Nonenmacher T (1991) Lecture Notes in Physics No. 38. Springer, Berlin, Heidelberg, New York, pp 321–330
16. Schlesinger MF (1988) Ann Rev Phys Chem 39:269–290
17. Tschoegl NW (1989) The Phenomenological Theory of Linear Viscoelastic Behavior – An Introduction. Springer, Berlin, Heidelberg, New York
18. Doi M, Edwards SF (1986) The Theory of Polymer Dynamics, Clarendon Press, Oxford
19. Oldham KB, Spanier J (1974) The Fractional Calculus. Academic Press, New York, London
20. Jambon F, Winter HH (1986) J Rheology 30:367–373
21. Friedrich Chr, Heymann L (1988) J Rheology 32:235–241
22. Schiessel H, Blumen A (1993) J Phys A 26:5057–5069

23. Ferry JD (1980) Viscoelastic Properties of Polymers, Wiley & Sons, New York
24. Bagley RL, Torvik PJ (1983) J Rheology 27:201–210
25. Glöckle WG, Nonnenmacher TF (1993) J Stat Physcis 71:741–757

Received December 1, 1993;
accepted April 5, 1994

Authors' address:

Dr. Christian Friedrich
Freiburger Materialforschungszentrum
Albert-Ludwigs-Universität Freiburg i. Br
Stefan-Meier-Str. 31A
79104 Freiburg i. Br. FRG